PRACTICAL THREE-DIMENSIONAL EFFECTIVE STRESS ANALYSIS CONSIDERING CYCLIC MOBILITY BEHAVIOR

Hiroyuki Yoshida[1], Kohji Tokimatsu[2], Tatsuya Sugiyama[3] and Tadahiko Shiomi[4]

[1] *Member, Arch. & Struct. Eng. Operation Center, Tokyo Electric Power Services Co., Ltd., Tokyo. Japan*
[2] *Professor, Dept. of Architecture and Building Engineering, Tokyo Institute of Technology, Tokyo. Japan*
[3] *Senior Researcher, R&D Center, Tokyo Electric Power Company, Kanagawa. Japan*
[4] *Assistant to General Manager, R&D Institute, Takenaka Corporation, Chiba. Japan*
Email: yoshida@tepsco.co.jp, kohji@o.cc.titech.ac.jp, shiomi.tadahiko@takenaka.co.jp, s.tatsuya@tepco.co.jp

ABSTRACT:

A number of effective stress analysis methods have been developed; however, they are often complex, requiring a number of parameters that are not easy to determine in practice of seismic design. A strong need, therefore, exists to develop a more practical method capable of simulating essential features such as liquefaction of the soil subjected to strong shaking. In this paper, a practical three-dimensional effective analysis coupled with a three-dimensional stress-strain model of sand is presented in which only soil properties obtained from a common field and laboratory test results. A key mechanism simulating liquefaction and cyclic mobility behavior is modeled based on the accumulated damage concept for pore pressure generation with a generalized hardening model for shear behavior. In addition, the composition rule that has been constructed for a one-dimensional shear stress-strain relation is extended to three-dimensional problems. To demonstrate the effectiveness of the proposed analysis, a large-scale field liquefaction test on soil-pile-structure models using blast-induced shaking is simulated. The computed results, including the acceleration and displacement responses of the structures, and the bending moment and axial stress in the piles as well as liquefaction and cyclic mobility behavior of the ground, are found to be in good agreement with the field test results. The good agreement suggests that the propose method, which requires soil parameters readily be obtained from common filed and laboratory tests, is convenient and yet effective in practice.

KEYWORDS: Three Dimensional Effective Stress Analysis, Cyclic Mobility, Large Scale Model Test

1. INTRODUCTION

It is important to consider the effects of soil liquefaction and cyclic mobility in the design of structures to be constructed on liquefiable soils. For this purpose, a number of effective stress analysis methods have been developed; however, they are often complex, requiring a number of parameters that are not easy to determine in practice. A strong need, therefore, exists to develop a more practical method capable of simulating essential features of the soil subjected to strong shaking. In this paper, a practical three-dimensional effective stress analysis coupled with a three-dimensional stress-strain model of sand is presented in which only soil properties obtained from a common field and laboratory test results, i.e., geological and geophysical logs, strain-dependent elastic shear modula and damping ratios, and liquefaction curve, are required as the input parameters.

2. CONSTITUTIVE MODEL

Figure 1 shows an example of soil liquefaction test of a soil specimen. The behavior of sand is greatly different before and after generating cyclic mobility as shown in Figure 1. Then, it separates different between early and latter phases (i. e., before and after initiation of cyclic mobility) during cyclic loading.
In addition, the composition rule that has been constructed for a one-dimensional shear stress-strain relation is extended to three-dimensional problems.

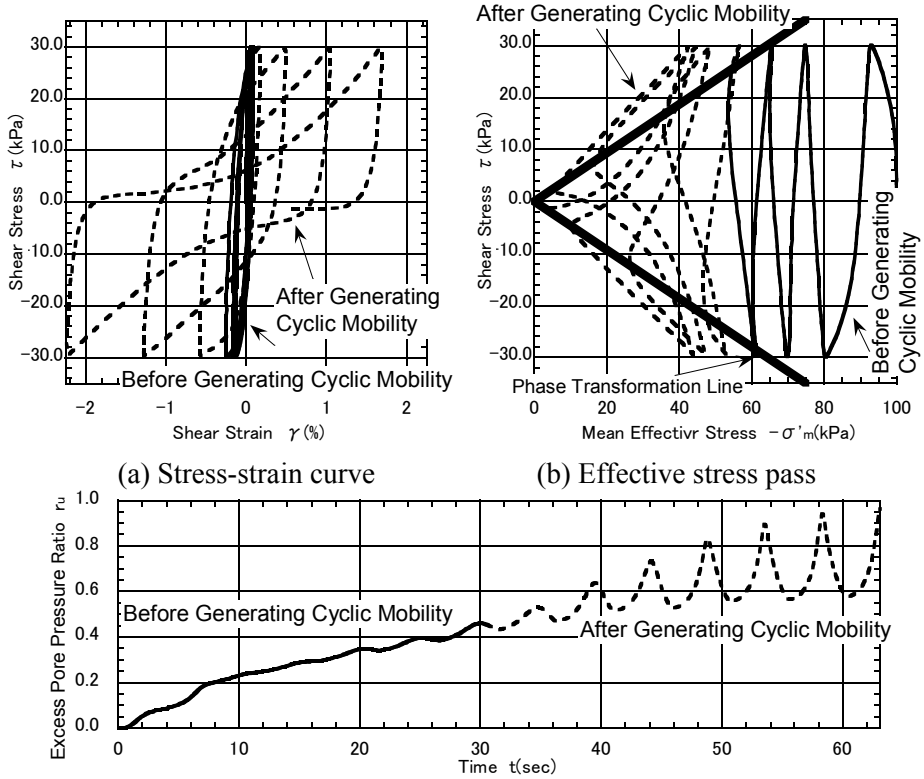

(a) Stress-strain curve (b) Effective stress pass

(c) Time history of excess pore water pressure ratio

Figure 1 Example of cyclic loading torsional shear test

2.1. Soil Behavior before Initiation of Cyclic Mobility

The shear stress τ can be expressed by:

$$\tau = G_0 \cdot \mathrm{f}(\gamma) \cdot \mathrm{g}(\sigma'_m) \tag{1}$$

in which τ = shear stress of soil, G_0 = initial elastic shear modulus, $\mathrm{f}(\gamma)$ = strain dependent elastic shear modulus ratio, $\mathrm{g}(\sigma'_m)$ = mean stress dependent elastic shear modulus ratio. Moreover, elastic shear modulus G_{m0} and shear strength $\tau_{\max}$ can be expressed by:

$$G_{m0} = G_{ref} \cdot (\sigma'_m / \sigma'_{ref})^n \tag{2}$$

$$\tau_{\max} = \sigma'_m \cdot \tan\phi_f + c \tag{3}$$

in which G_{m0} = initial elastic shear modulus when mean stress equals σ'_m, G_{ref} = initial elastic shear modulus when mean stress equals σ'_{ref}, $\tau_{\max}$ = shear strength when mean stress equals σ'_m, σ'_m = mean stress, σ'_{ref} = reference mean stress, n = parameter, ϕ_f = friction angle, c = cohesion.

2.1.1 Hardening Model for Shear Behavior

The nonlinearity rule of soil is often shown by the dynamic strain dependent characteristic, i.e., G/G_0 - γ curve and h - γ curve. It is because the curves can be examined directly by cyclic triaxial tests or cyclic torsional test. Moreover, it is because the equivalent linear analysis SHAKE of which the input data was the characteristic was used. A lot of research and proposals have been made for developing an analytical method that uses the dynamic strain dependent characteristic for a truly nonlinear analysis so far. The typical one is the hyperbolic model and Ramberg-Osgood model. However, these analytical methods need modeling for the skeleton curve where the dynamic strain dependent characteristic is shown by some analytical parameters. Therefore, the fitting of the dynamic strain dependence characteristic cannot be done at the all magnitudes of strain. Engineering judgment is needed as to which strain level to show by the problem of targeting it.

Yoshida et al. (1990) proposed an analytical method that defines the skeleton curve directly as a partial linear function from the curve, aiming to assume only soil properties obtained from a common field and laboratory test results to be an analytical parameter as shown in Figure 2. In addition, a fictitious skeleton curve is

defined by the hyperbolic function so that the hysteresis damping obtained from the hysteresis curve per cycle and the one obtained from h-γ curve become equal. The stress-strain relationship at each cycle can be completely matched to the dynamic strain dependence characteristic by using this analytical method. This method was chosen to be used as a hardening model for shear behavior in the method proposed in this study.

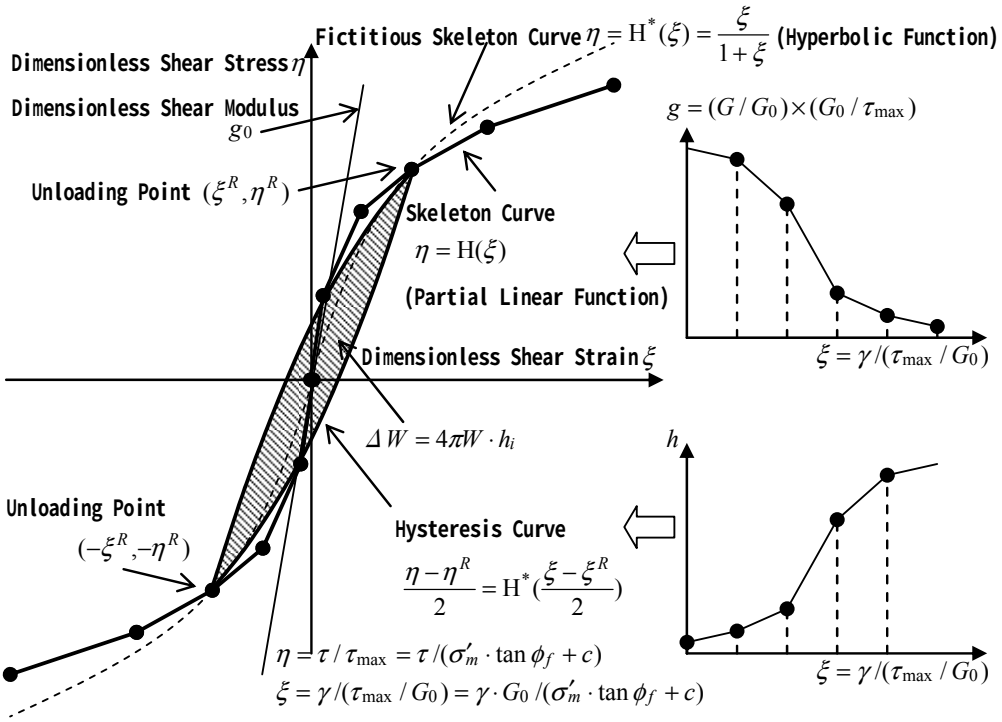

Figure 2 Modeling of nonlinearity for shear strain behavior

2.1.2 Evaluation Method of Excess Pore Water Pressure Ratio

The liquefaction characteristic of the sand subjected to cyclic loading is often shown in the liquefaction strength curve. This is because the liquefaction strength curve can be examined directly by triaxial test or torsional test as well as the dynamic strain dependence characteristic. A lot of research and proposals have been made for developing an analytical method that uses the liquefaction strength curve for an effective stress analysis. The basic method is to construct the mathematical model constructed to be able to simulate general behavior at liquefaction, and is used an analytical parameter where the liquefaction strength curve can be reproduced based on engineering judgment.

Recently, Shiomi et. al.(2005) have developed an analytical method CWELL to which behavior was able to be evaluated without needing an advanced engineering judgment, and assuming only the soil properties obtained from common field and laboratory test results to be directly used as input data of the calculation. In this method, the damage parameter $\Delta D_{(i)}$ of soil during liquefaction is calculated from the maximum shear stress ratio $\tau_{max(i)}/\sigma'_{m0}$ and the liquefaction strength curve in a half cycle of i-th turn as follows:

$$\Delta D_{(i)} = 1/2N_{f(i)} \tag{4}$$

in which $N_{f(i)}$ = a number of cycles where liquefaction is generated by shear stress ratio $\tau_{max(i)}/\sigma'_{m0}$. As shown in Figure 3, the accumulated damage parameter obtained by this increment of the damage parameter $\Delta D_{(i)}$ accumulates to a half cycle of n-th turn is calculated as follows:

$$D_{(n)} = \sum_{i=1}^{n} \Delta D_{(i)} \tag{5}$$

in which $D_{(n)}$ = an accumulated damage parameter at n-th turn.

Unlike the real soil behavior in the laboratory, the excess pore water pressure ratio changes discontinuously in the CWELL method as understood from Figure 4. Then, an increase of excess pore water pressure ratio in a

half cycle is continuously evaluated in this law as follows. The accumulated damage parameter at time t_{n+k} in the half cycle of n-th turn is defined by:

$$D_{n+k} = \sum_{i=1}^{n-1} \Delta D_{(i)} + \Delta D_{(n,k)} \tag{6}$$

in which $\Delta D_{(n,k)}$ = an increment of the damage parameter till time t_{n+k} in the half cycle of n-th turn.

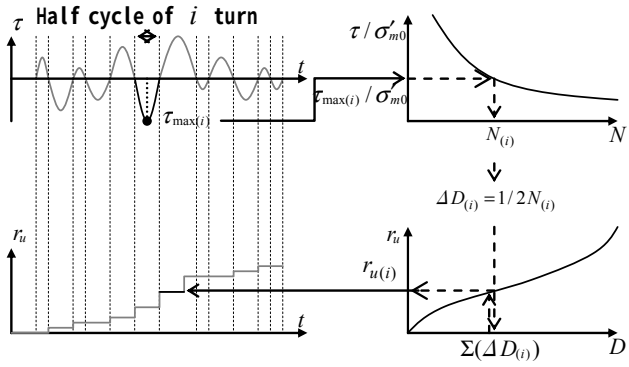

Figure 3 Evaluation method of excess pore water pressure ratio in CWELL method

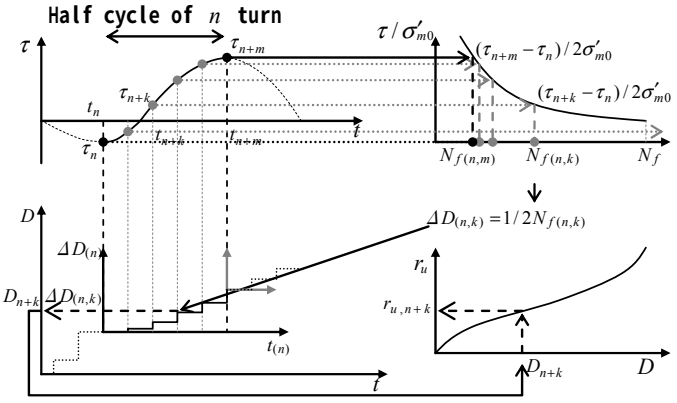

Figure 4 Evaluation method of excess pore water pressure ratio in proposal method

2.2 Soil Behavior after Initiation of Cyclic Mobility

The soil behavior after initiation of cyclic mobility may be separated into two phases: one is the section from the phase transformation line to the unloading point and the other is the one from the unloading point to the phase transformation line, and the nonlinearity is evaluated.

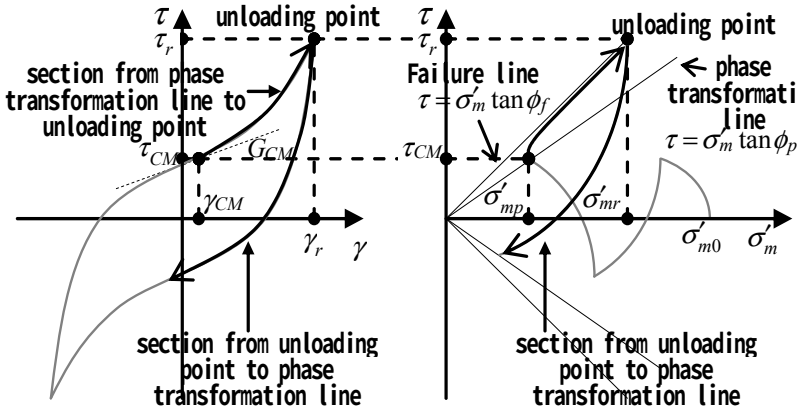

(a) Stress-strain curve (b) Effective stress path

Figure 5 Soil behavior after initiation of cyclic mobility

2.2.1 The Section from the Phase Transformation Line to the Unloading Point

For the section from the phase transformation line to the unloading point, the tangent elastic shear modulus G_T is calculated from mean effective stress σ'_m and the maximum shear strain $\gamma_{\max}$ experienced till then by using the empirical formula (7)-(10) obtained from the study of the laboratory test results.

$$G_T = G_{CM} + f_b \cdot \frac{\sigma'_m - \sigma'_{mp}}{\sigma'_{m0}} \cdot G_{m0} \tag{7}$$

$$G_{CM} = G_{m0} \cdot 10^{6(\sigma'_{mp}/\sigma'_{m0})^{0.15} - 6.6} \tag{8}$$

$$f_b = 5b \cdot \exp(-40 \cdot \gamma_{\max}) + b \tag{9}$$

$$b = 350 \cdot (G_{m0}/\sigma'_{m0})^{-1.4} + 0.045 \tag{10}$$

in which G_{CM} = a tangent elastic shear modulus when effective stress path crosses the phase transformation line, f_b = an increase rate of G_T, b = parameter.

It is considered that the stress point is asymptotic from the phase transformation line in the failure line according to an increase in the shear stress, and the mean effective stress is calculated by:

$$\sigma'_m = \frac{1}{\tan\phi_f} \cdot \frac{|\tau/\tau_{\max}| - M_0}{1 - M_0} \cdot \tau \tag{11}$$

in which σ'_m = mean effective stress, τ = shear stress, $\tau_{\max}$ = shear strength, $M_0 = \tan\phi_p / \tan\phi_f$, ϕ_f = friction angle, ϕ_p = phase transformation angle.

2.2.2 The Section from the Unloading Point to the Phase Transformation Line

The initial elastic shear modulus is calculated by the same equations (2) and (3) defined for the soil characteristics before cyclic mobility. Moreover, mean effective stress is calculated from shear stress by using the effective stress path expressed by the empirical formula (12) obtained from the study of the laboratory test results.

$$\frac{\sigma'_m - \sigma'_{mr}}{\sigma'_{mp} - \sigma'_{mr}} = \sin\left\{\frac{\pi}{2} \cdot \left(\frac{\tau - \tau_r}{\tau_p - \tau_r}\right)^{1.2}\right\} \tag{12}$$

in which σ'_{mr}, τ_r = a mean effective stress and shear stress at unloading point, σ'_{mp}, τ_p = a mean effective stress and shear stress effective stress path crosses the phase transformation line, σ'_m, τ = a current mean effective stress and shear stress.

2.3 Extension to Three-Dimensional Problems

The composition rule previously described is constructed for one dimensional problem. It is necessary to extend this composition rule to a three-dimensional problem. The relationship between shear stress τ and shear strain γ in the one-dimensional problem is given as the relationship between equivalent stress σ_e and equivalent strain e in a three-dimensional problem. Thus, the degree of nonlinearity is evaluated based on the increment of equivalent stress from the unloading point in this composition rule as shown in Figure 7, according to the study by Yoshida, in which η_{ij} = a dimensionless equivalent stress $\sigma_e / \tau_{\max}$, $\eta_{ij,R}$ = a dimensionless equivalent stress at unloading point

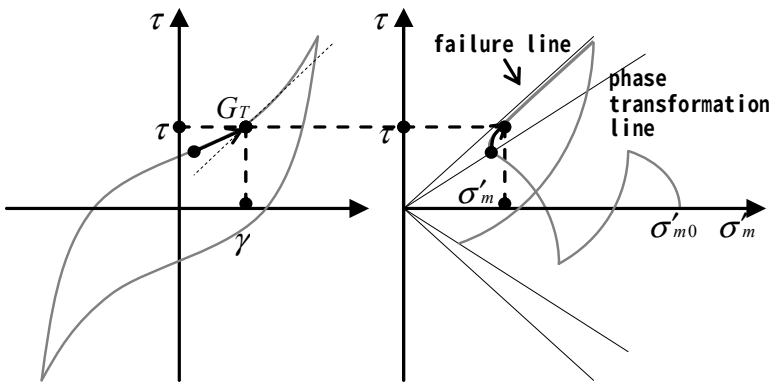

Figure 6 Tangent elastic shear modulus G_T

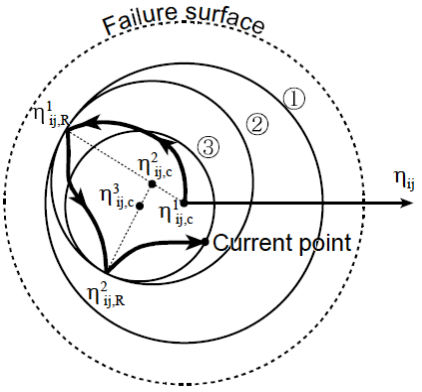

Figure 7 Increment of equivalent stress

3. VERIFICATION ANALYSIS

The vibration tests of pile supported structure in liquefiable sand were simulated to confirm the effectiveness of the proposed composition rule in performance design. The result is shown as follows.

3.1 Outline of vibration tests and response of soil-pile-structure

The vibration tests were executed in the Black Thunder Coal Mine in the United States state of Wyoming. To

remove mudstone on the coal layer, a large-scale blast was done though the coal mining is executed in this mine by a method near open-pit. The excitation experiment of the pile supported structure by the large input from the bedrock was done by using the ground vibration generated in that case. Figure 8 shows the outline of the vibration test. The test setup including a structure model in a backfill of saturated sand. The backfill had a ground dimension of 12mx12m, bottom 6m×6m, and 3m in depth. The waterproof layer was set up on the bottom and the slope of the backfill, it was filled with the saturated sand. The piles were the steel pipe paling of about 32cm in diameter, about 1cm in thickness, and 3.7m in length. The top slab and the base slab made of reinforced concrete had a square dimension of 3mx3m with a thickness of 50 cm. Figure 9 shows the outline of the structure model.

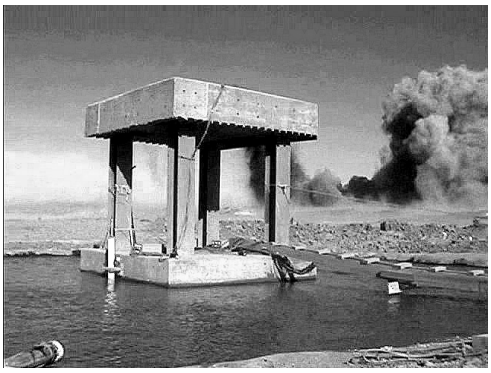

Picture 1 Test situation

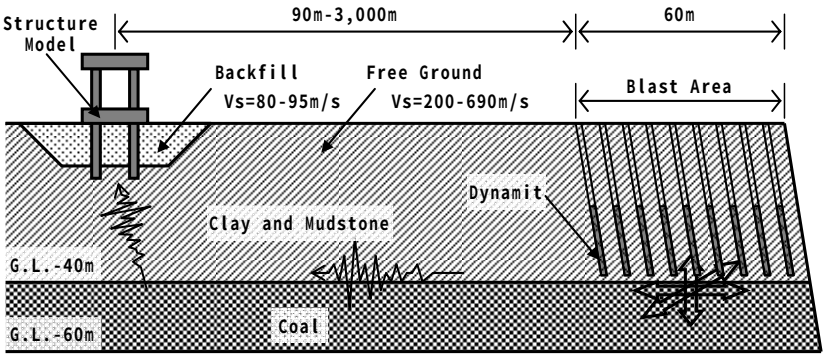

Figure 8 Outline of vibration test

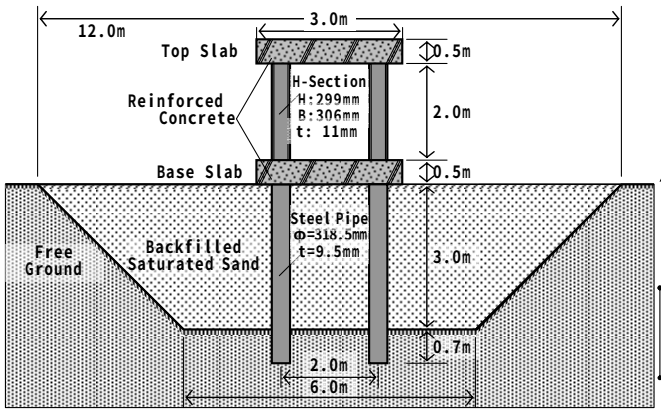

Figure 9 Outline of structure model

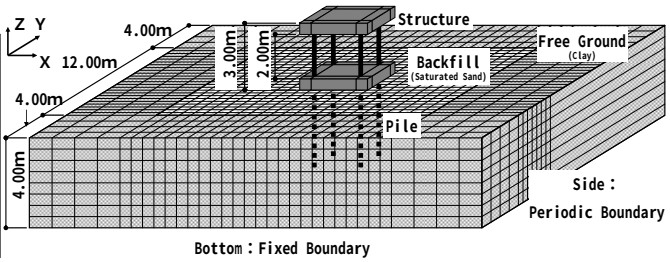

Figure 10 3-dimensional FEM model

3.2 Test Model

An analytical model is three dimensional FEM shown in Figure 10. Table1 and Figure 11 show the model parameters obtained from a common field and laboratory test results.

The observed record at G.L.-4m in the free ground 18 m away from the edge of the backfill, as shown in Figure 12, was used as the input within motion (i.e., E+F waves) to the base of the FEM model.

Table1 Material parameters for numerical simulation

	S-wave Velocity Vs (m/s)	P-wave Velocity Vp (m/s)	Poisson Ratio ν_d	Density of Soil γ (t/m^3)	Density of Water γf (kN/m^3)	Bulk Modulus of Soil Ks (kN/m^2)	Bulk Modulus of Water Kf (kN/m^2)
Free Ground	215	480	0.37	1.67	—	—	—
Backfill	80	1530	0.33	1.89	9.81	1.0E+10	2.2E+6

	Shear Modulus of Soil G (kN/m^2)	Referencee Pressure σ_{ref} (kN/m^2)	Cohesion c (kN/m^2)	Internal Friction Angle Φ_f (°)	Phase Transformation Φ_p (°)	Porosity n	Permeability k (m/s)
Free Ground	77196	41.00	130	0	—	—	—
Backfill	12096	13.80	0	17.44	17.27	0.44	1.00E-5

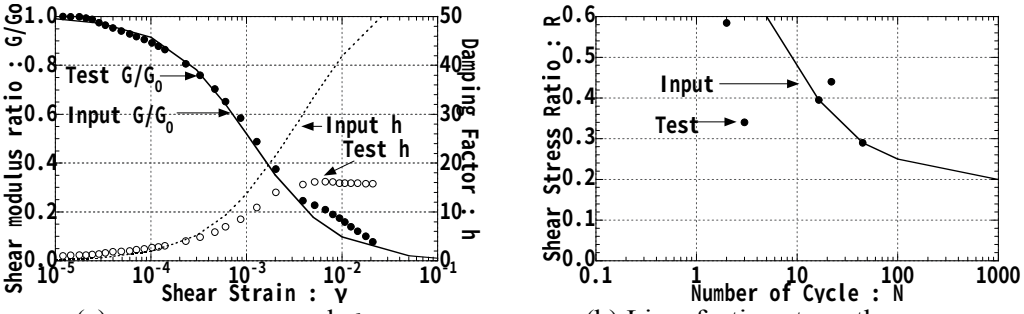

(a) G/G_0 - γ curve and h - γ curve (b) Liquefaction strength curve

Figure 11 Laboratory test results for backfilled sand

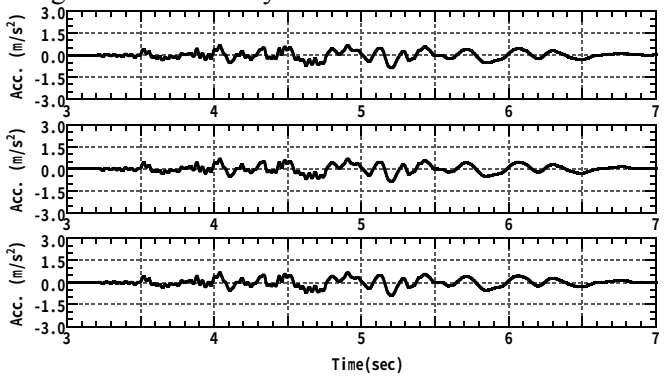

Figure 12 Input motion(Observed record at G.L.-4.0m in the free ground)

3.3 Comparison of Model Test and Analysis

Figure 13 and Figure 14 show the acceleration time histories on the surfaces of the free field and the backfill. Analytical results of free ground are in good agreement with the observed record well because the free ground was almost in the range of elasticity. Figure 15 shows the excess pore water pressure time history at G.L.-1.4m in the backfill. It reached the initial effective stress at 4.5 seconds. A good agreement in acceleration time histories is found between computed and observed ones, confirming the effectiveness of the proposed method. The wave of the high frequency is seen, and it is thought that the shear modulus of soil at liquefaction is evaluated a little high after 4.5 seconds.

Figure 16 shows the acceleration time history on the base slab. The response of structure at completely liquefied time is in good agreement with the one of the ground. In addition, the one of the structure after complete liquefaction is also in good agreement. Moreover, the computed curvature time history at the pile head after complete liquefaction could simulate well the observed one. It is conceivable that the influence of the difference of the shear modulus of soil at liquefaction is small from the point of response evaluation of the structure.

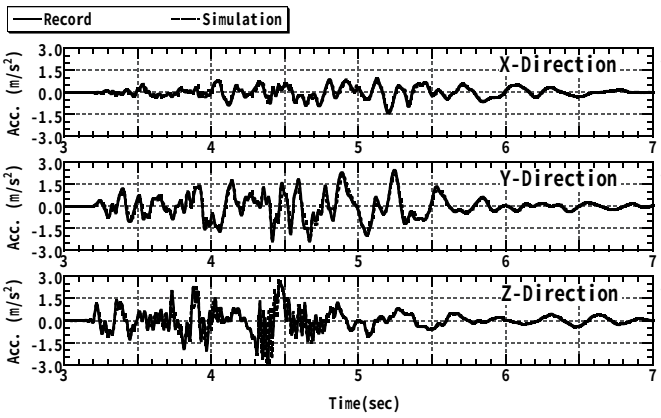

Figure 13 Acceleration on the surface of the free ground

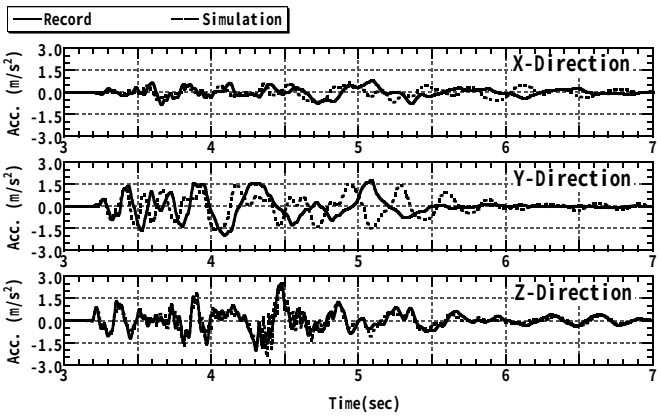

Figure 14 Acceleration on the surface of the backfill

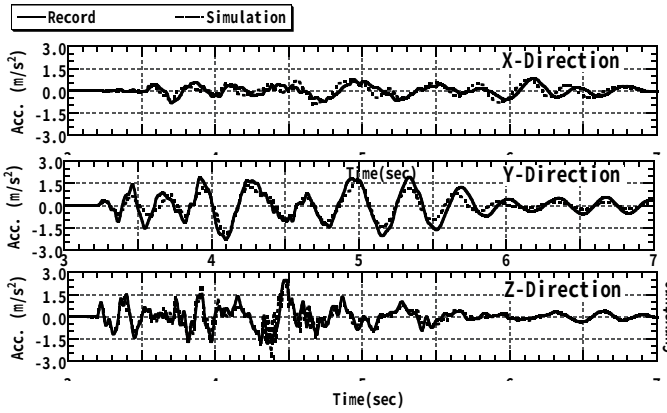

Figure 16 Acceleration time history on the base slab

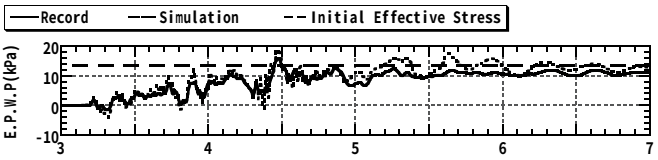

Figure 15 Excess pore water pressure at G.L.-1.4m

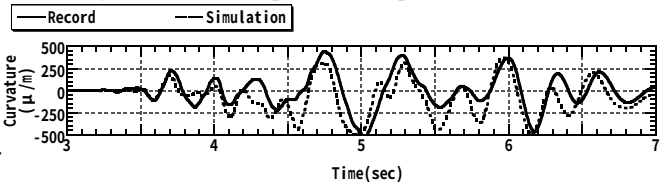

Figure 17 Curvature time history at the pile head

4. CONCLUSIONS

In this paper, a practical three-dimensional effective stress analysis coupled with a three-dimensional stress-strain model of sand is presented in which only soil properties obtained from a common field and laboratory test are required. To demonstrate the proposed method is verified, records of vibration tests of pile-supported structure in liquefiable sand using large-scale blast are simulated. The computed results are found to be in good agreement with observed records. The good agreement suggests that the proposed method, which requires soil parameters readily obtained from common filed and laboratory tests as input, is convenient and yet effective in practice.

REFERENCES

Yoshida,H., Tokimatsu,K., Hijikata,K., et al. (2006), "Study on practicable 3-dimensional effective stress analysis using the ground survey result," *Summaries of Technical Papers of Annual Meeting Architectural Institute of Japan*, **B-1**, 623-626.

Yoshida,H., Tokimatsu,K., Hijikata,K., et al. (2007), "Study on influence of multi-dimensional input by three-dimensional effective stress analysis," *Summaries of Technical Papers of Annual Meeting Architectural Institute of Japan*, **B-1**, 539-540.

Yoshida,H., Tokimatsu,K., and Sugiyama,T. (2007), "Simulation of full-scale model test by practicable, three-dimensional effective stress analysis," *Proceedings of the 5th Annual Meeting of Japan Association for Earthquake Engineering*, 176-177.

Yoshida,N., Tsujino,S., and Ishihara,K. (1990), "Stress-strain model for nonlinear analysis of horizontally layered deposit," *Summaries of Technical Papers of Annual Meeting Architectural Institute of Japan*, **B**, 1639-1640.

Shiomi,T., Tokimatsu,K., et al. (2005), "Equivalent linear analysis taking into account excess pore water pressure built-up due to liquefaction," *Journal of structural and construction engineering. Transactions of AIJ*, **No.598**, 93-100.

Yoshida,N., Tsujino,S., et al. (1993), "A simplified practical stress-strain model for the multi-dimensional analysis under repeated loading," *The 28th Japan National Conference on Soil Mechanics and Foundation Engineering*, 1221-1224.

Saito,H., Tanaka,H., et al. (2002), "Vibration tests of pile supported structure in liquefiable sand using large-scale blast -Outline of vibration tests and response of soil pile-structure-," *J. Struct. Constr. Eng., AIJ*, **No.553**, 41-48.

Saito,H., Tanaka,H., et al. (2002), "Vibration tests of pile supported structure in liquefiable sand using large-scale blast -Simulation analysis for vibration tests of soil-pile-structure-," *J. Struct. Constr. Eng., AIJ*, **No.557**, 85-92.